# OVERCOMING SENSITIZATION IN WELDS USING FeCrAl ALLOYS

R. B. REBAK, V. K. GUPTA, M. DROBNJAK, D. J. KECK,* E. J. DOLLEY
*GE Global Research, 1 Research Circle, Schenectady, NY 12309, USA*
**GE Hitachi Nuclear Energy Americas, Wilmington, NC, 28402, USA*

## ABSTRACT

For the last six years the international nuclear fuels community has been involved in finding a fuel that would resist a severe plant accident (such as complete loss of coolant). One of the solutions, championed in the US by General Electric and Oak Ridge National Laboratory is to replace the zirconium cladding for the urania fuel using a ferritic IronClad iron-chromium-aluminum (FeCrAl) alloy. The FeCrAl alloys are iron based and may contain 10-21% Cr, 4-6% Al, 2-3% molybdenum and minor amounts of rare earth elements and zirconium. The FeCrAl were selected for their outstanding resistance to corrosion both under normal operation conditions (e.g. high purity water near 300°C) and under accident conditions (e.g. steam at T>1200°C). Austenitic stainless steels (SS) have been used before as cladding for the fuel but they were abandoned in the last few decades mainly due to their weld associated cracking from the coolant side. Sensitization produced in higher carbon austenitic stainless steels a chromium depleted path for environmental cracking. Ferritic alloys are highly resistant to stress corrosion cracking in simulated light water reactor environments. However, until now there is no information if the FeCrAl would sensitize during welding procedures. Current results show that IronClad alloys did not experience sensitization or other phase transformation during thermal exposures of 677°C for 2 h or 732°C for 1 h.

### INTRODUCTION

There has not been much innovation in nuclear materials in the last few decades [1]. The accident at the Fukushima nuclear power stations in March 2011 precipitated a worldwide resurgence in materials research to find a replacement for the classic fuel rod made of zirconium alloy cladding and urania fuel. The hydrogen explosions at the Fukushima power stations suggested an alternative for zirconium, which may exothermically react (oxidize) rapidly in water and steam at temperatures above operation conditions to release hydrogen gas. One of the solutions proposed by General Electric (GE) and Oak Ridge National Laboratory (ORNL) is to replace the zirconium cladding using an IronClad ferritic iron-chromium-aluminum (FeCrAl) alloy. The FeCrAl alloys are iron based and may contain 10 to 21% Cr, 4 to 6% Al, smaller amounts of molybdenum (2-3%) and minor amounts of rare earth (RE) elements plus zirconium. The FeCrAl alloys were selected for their outstanding resistance to corrosion both under normal operation conditions (e.g. high purity water near 300°C) and under accident conditions (e.g. steam at T>1200°C) [2,3]. Under normal conditions, in hot water, FeCrAl resists corrosion by developing a few nanometers thick chromia film on the surface. Under accident conditions the chromia would evaporate as a volatile hydroxide and FeCrAl will be protected by less than a micrometer thick alumina film [4].

Austenitic stainless steels (SS) have been used before as cladding for the fuel but they were abandoned in the last few decades [1]. One of the reasons was that due to their higher carbon content, the austenitic stainless steels were thermally sensitized during welding and this made them vulnerable to intergranular stress corrosion cracking (IGSCC) from the coolant side, especially under oxidizing conditions [5]. Since thermally sensitized induced cracking not only happened in fuel cladding, the use of austenitic stainless steels for

other light water reactors components was partially resolved by using low carbon materials (less than 0.03%C) or by using stabilized alloys such as 321SS or 347SS [5].

Ferritic stainless steels and FeCrAl were never used before as reactor internal components for light water reactors, therefore, its characterization in reactor environments is important. It has been shown before that ferritic alloys with chromium are highly resistant to stress corrosion cracking in simulated light water reactor environments [6]. However, until now there is no information if FeCrAl alloys would sensitize during welding procedures.

The objective of the current work is to investigate the susceptibility of IronClad FeCrAl alloys to chrome depletion at grain boundaries during temperature excursions in the range 650 to 750°C, and to compare their behavior to the well-known sensitization phenomenon of austenitic type 304H SS. In future studies, the performance of ferritic FeCrAl alloys may be compared against stabilized SS), such as 321SS and 347SS, which contain carbon affinity elements Ti & Nb.

## EXPERIMENTAL PROCEDURE

In the current study, Type 304H austenitic SS (baseline) and ferritic IronClad FeCrAl alloys (APMT and C26M) (Table 1) were used. Traditionally melted and thermo-mechanically processed Type 304H SS and powder-metallurgy (hot-isostatic-pressed) APMT were procured in fully recrystallized, mill-annealed condition. C26M alloy was obtained in the warm-extruded rod form. Further details on the processing of APMT are not known due to proprietary nature. All materials were heat treated at 677°C for 2 h and at 732°C for 1 h, and their susceptibility to chromium depletion and sensitization behavior was evaluated using metallographic, electron microscopy and electrochemical techniques.

SEM characterization was performed using a Hitachi SU70 FEG-SEM with high resolution backscattered electron (BSE) imaging using BSE solid state diode (PDBSE) detector and energy dispersive spectroscopy (EDS) analysis was performed with Bruker XFlash 6 60mm² SDD EDS detector with Esprit 1.9.4 EDS software.

Electrochemically, the sensitization was assessed using the double loop electro-potential reactivation (EPR) test [7,8]. Tests were conducted in 0.5 M $H_2SO_4$ + 0.01 M KSCN solution, naturally aerated, room temperature. This test involved a potentiodynamic scanning at 1.67 mV/s in the anodic direction from the corrosion potential ($E_{corr}$, usually -400 mV SCE) until a potential of +0.3V SCE, then the scan direction is reversed in the cathodic direction until the original $E_{corr}$ is reached. The degree of sensitization (DOS) is measured by the ratio $i_a/i_r$, where $i_a$ and $i_r$ are the current peaks in the forward and reverse directions, respectively. Other tests included the monitoring of the corrosion potential and polarization resistance scanning (ASTM G59) (not included in this manuscript).

Table 1. Nominal Compositions of FeCrAl (in mass percent, balance is Fe).

| Alloy | Cr | Al | Others |
|---|---|---|---|
| 304H SS | 18 | None | 8Ni + 0.06C + 1.8Mn |
| APMT | 21 | 5 | 3Mo |
| C26M | 12 | 6 | 2Mo + 0.05Y + 0.007C |

## EXPERIMENTAL RESULTS

Figure 1 shows the double loop tests for baseline type 304HSS, in the as received (AR) and in the heat treated (HT) condition of 677°C for 2h. This temperature and time heat treatment was selected following the guidelines in Ref. 7, which were later incorporated into ASTM and ISO standards. These heat treatment conditions were chosen to simulate temperature and time generally observed in the TIG welding process (i.e., melting and cooling), and also to compare APMT and C26M alloys with the baseline 304H SS, which has

been evaluated earlier for sensitization under similar conditions as reported by Majidi and Streicher [7]. In the forward scan both AR and HT materials show a peak ($i_a$) but in the reverse scan only the HT material showed the peak ($i_r$). For type 304H HT at 677°C for 2 h, the DOS = $i_r/i_a$ = 7.381 mA/33.21 mA = 0.22 (sensitized), but for the AR condition, $i_r/i_a$ = 0.054 mA /30.93 mA = 0.001 (not sensitized) [7]. (In the absence of peak current in the reverse scan for the AR 304H SS, the $i_r$ was taken as the current at the potential of the anodic peak in the forward direction). Figure 2 shows the double loop tests for APMT alloy, also under AR and thermally aged at 677°C for 2 h conditions and tested in 0.5 M $H_2SO_4$ + 0.01 M KSCN at ambient temperature. Figure 2 shows that both the AR and thermally treated APMT specimens did not show the reactivation peak in the reverse scan. That is, APMT does not get thermally sensitized in the same manner as the higher carbon type 304H SS, as shown in Figure 1. Results for the electrochemical reactivation (EPR) tests for C26M are illustrated in Figure 3, which shows that both the AR and thermally treated specimens exhibited the same behavior. Results from Figure 3 suggest that the current EPR test may not be the most appropriate test method for the lower Cr alloy C26M (Table 1), since the concentration of Cr in C26M is only 12%. The EPR method was developed for Type 304 SS, which has a higher Cr content (≥ 18%). In type 304SS, during sensitization, the Cr content may drop from 18% to 12% depletion regions adjacent to grain boundaries, which is detected with the EPR corrosion test as a degree of sensitization (DOS). In contrast, since the base composition of C26M is already 12%, the EPR used electrolyte may not be suitable for C26M or other materials with lower amount of Cr.

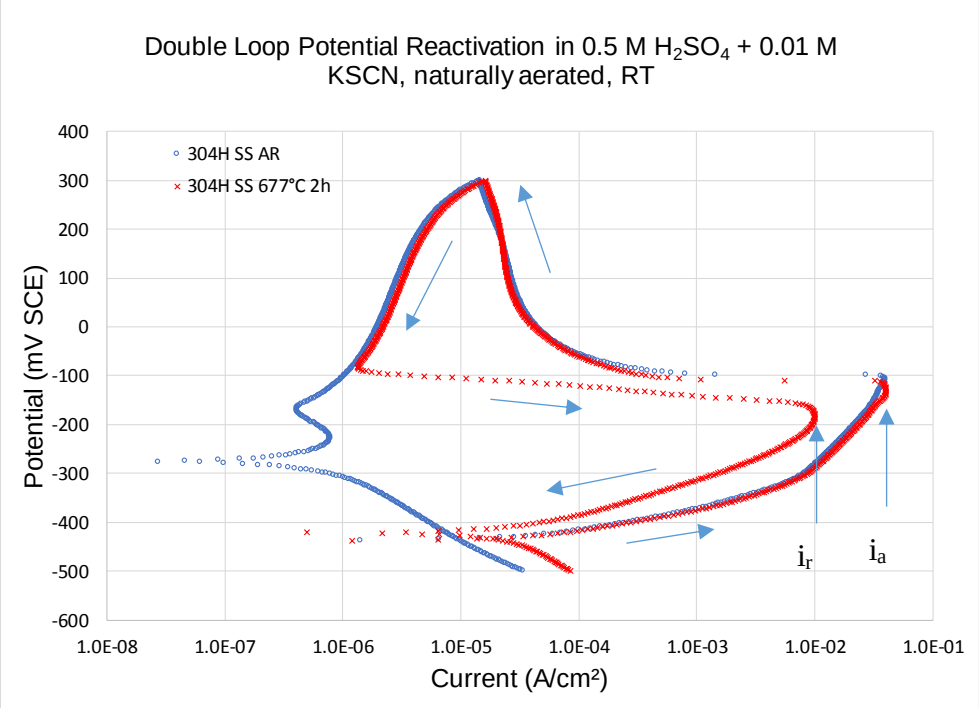


**Figure 1**. Double loop electro-potential reactivation (EPR) tests showing the behavior of 304H SS in the as-received (AR) non-sensitized (blue line) vs. a 2 h thermal treatment at 677°C or sensitized (red line).

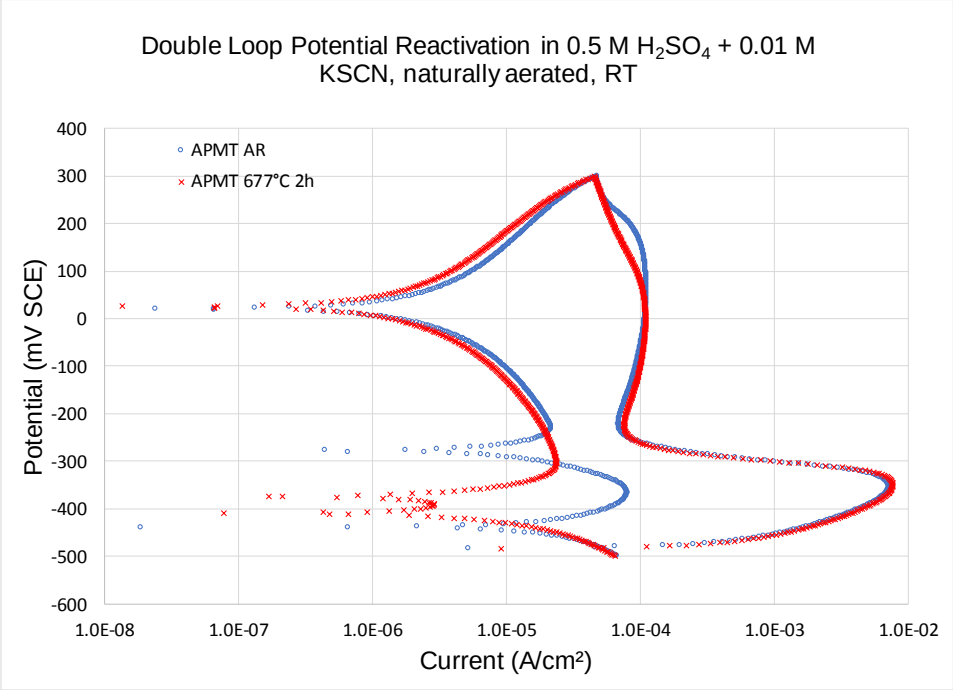


**Figure 2**. Double loop electro-potential reactivation tests for APMT in the as-received non-heat treated (blue line) vs. a 2 h thermal treatment at 677°C (red line). The heat treated APMT specimens did not show the anodic reactivation peak in the reverse scan as the 304H SS in Figure 1, implying that APMT does not suffer sensitization.

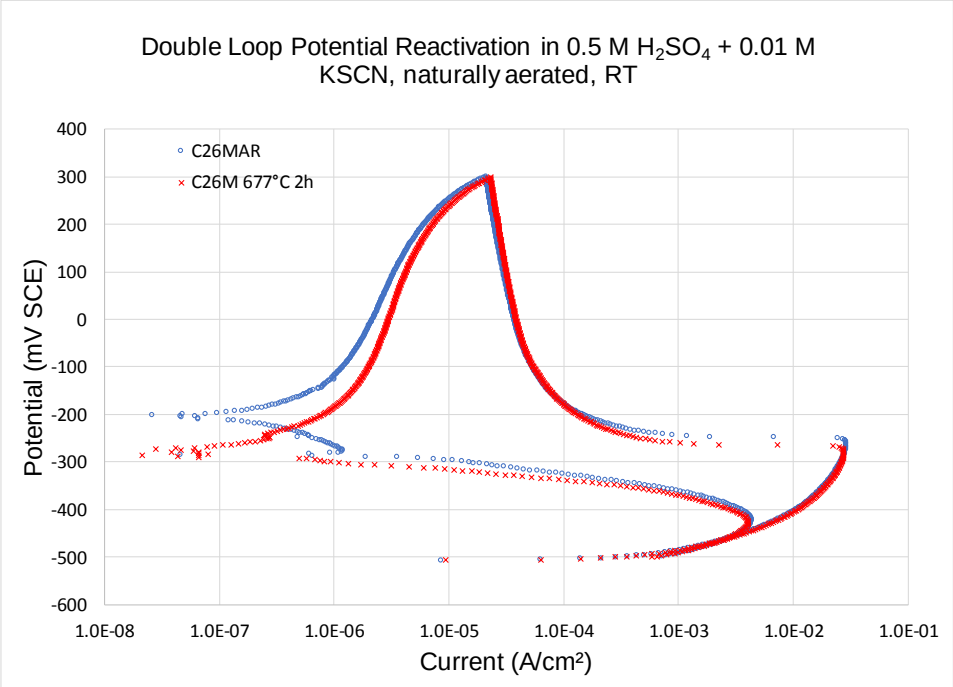


**Figure 3**. Double loop electro-potential reactivation tests for C26M in the as-received non-heat treated (blue line) vs. a 2 h thermal treatment at 677°C (red line). Both the AR and heat treated C26M specimens showed identical behavior. Results show that the EPR test may not be suitable for C26M because it has a low Cr content of 12%.

Figure 4 shows the as-received metallographic analyses of the three alloys, Type 304H SS, C26M and APMT alloys, in the as-received conditions. In general, the austenitic material had larger grains than the ferritic materials. APMT showed abundant nano-sized second phase particles (shown as white), which are rich in elements such as Y, Zr, Hf and Ti. Other particles in APMT are rich in Al and O. As-received C26M material showed partially recrystallized microstructure, likely due to highly retained plastic strain resulted from a warm-extrusion process. All three alloys show mainly clean grain boundaries in the higher magnification SEM images.

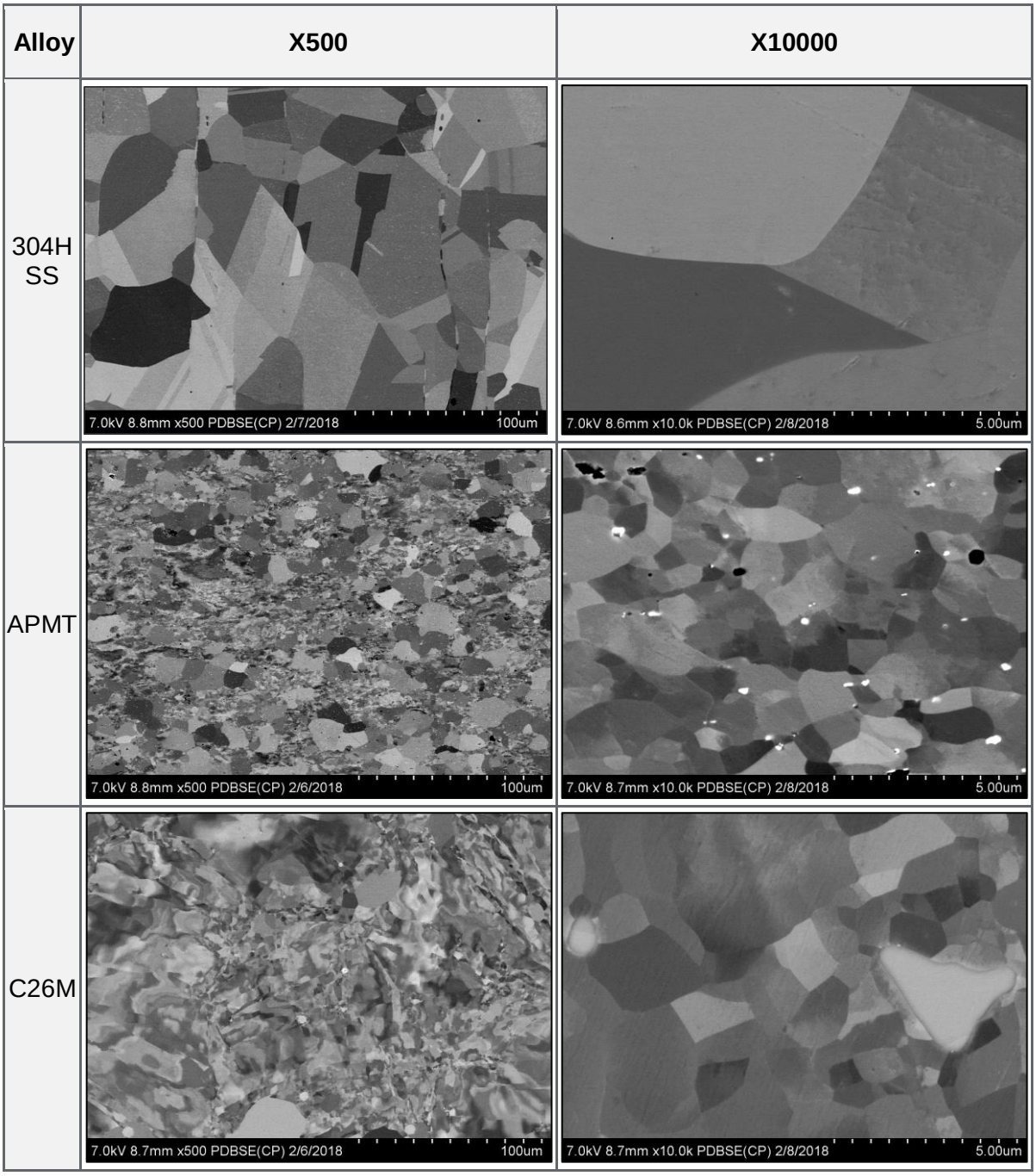


**Figure 4**. As-received microstructures of type 304H SS, C26M and APMT at X500 and X10,000 magnifications.

| Alloy | 677°C, 2h, X10,000 | 732°C, 1h, X10,000 |
|---|---|---|
| 304H SS | 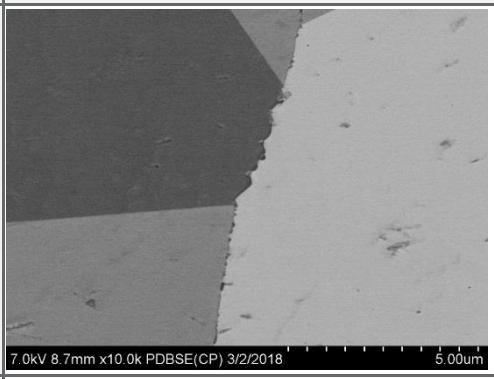  | 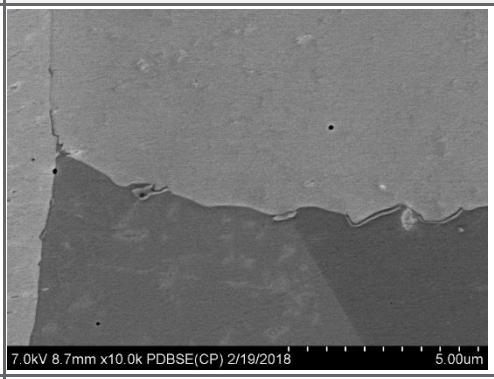  |
| APMT | 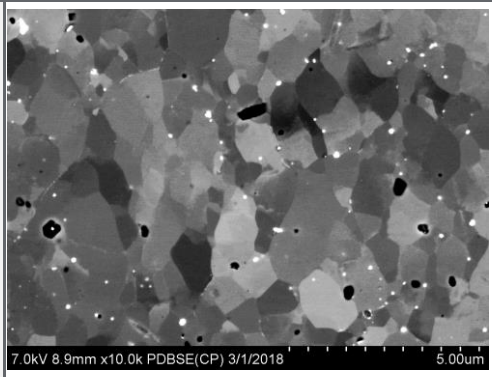  | 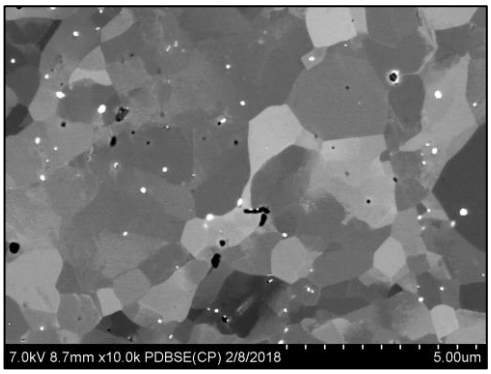  |
| C26M | 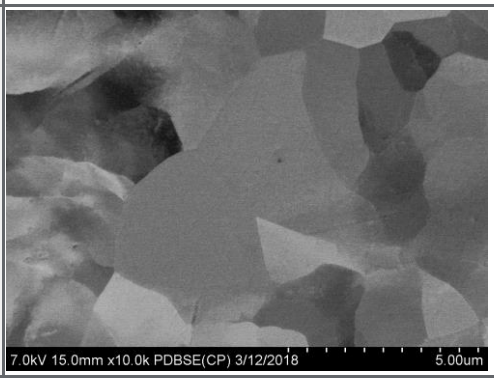  | 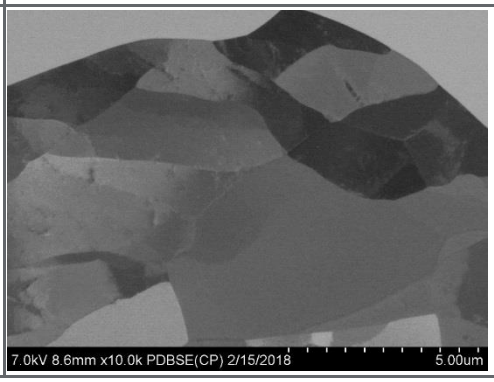  |

**Figure 5**. Thermally treated (677°C for 2 h and 732°C for 1 h) microstructures of type 304H SS, C26M and APMT at X10,000 magnification.

Figure 5 shows the metallographic analyses of Type 304H SS, C26M and APMT, heat treated at 677°C for 2 h and at 732°C for 1 h. In general, the grain boundaries of both ferritic APMT and C26M appeared clean and mostly free of precipitates. Figures 6 and 7 are EDS maps taken at 15kV accelerating voltage showing the presence of Cr and C rich precipitates at the grain boundaries for 304H SS. These are secondary carbides formed during the thermal treatment at 677°C and 732°C. During the formation of the secondary carbides, the vicinity of grain boundaries gets depleted in Cr causing the sensitization of the alloy, as shown in the anodic current peak in the reverse scan in Figure 1. APMT may also have sporadic and larger Cr and C rich precipitates in between grains (Figures 6 and 7); however, it is likely that those are primary carbides (including Mo carbide). These primary carbides at grain boundaries in APMT did not form during the thermal treatment, but probably during the manufacturing of the alloy. These carbide phases do not produce a Cr depleted region near the grain boundaries as evidenced by the EPR tests in Figure 2. Note that Cr and O peaks overlap, and thus, it is difficult to differentiate these elements using EDS maps.

| Alloy | 677°C, 2h, X15,000 |
|---|---|
| 304H SS | 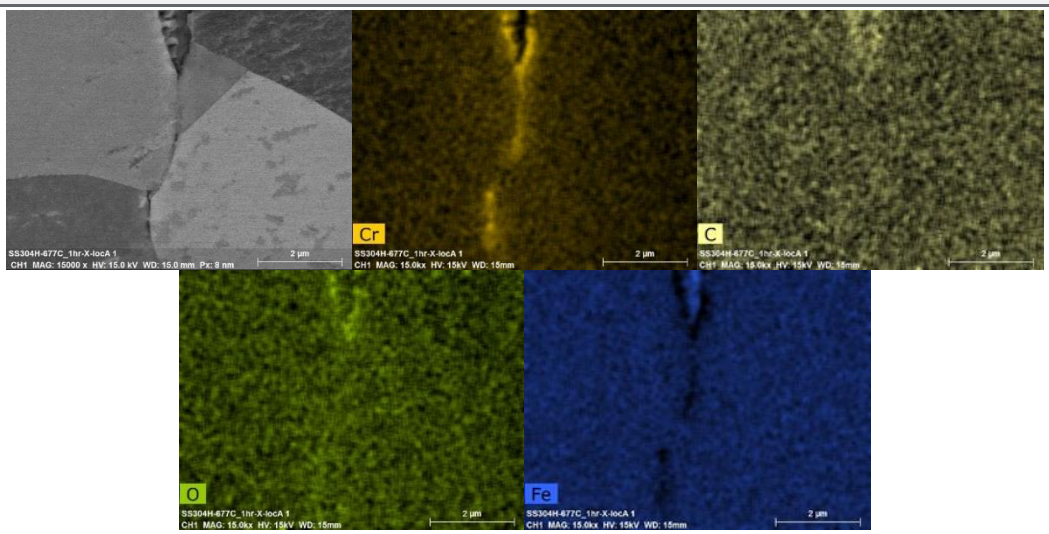  |
| APMT | 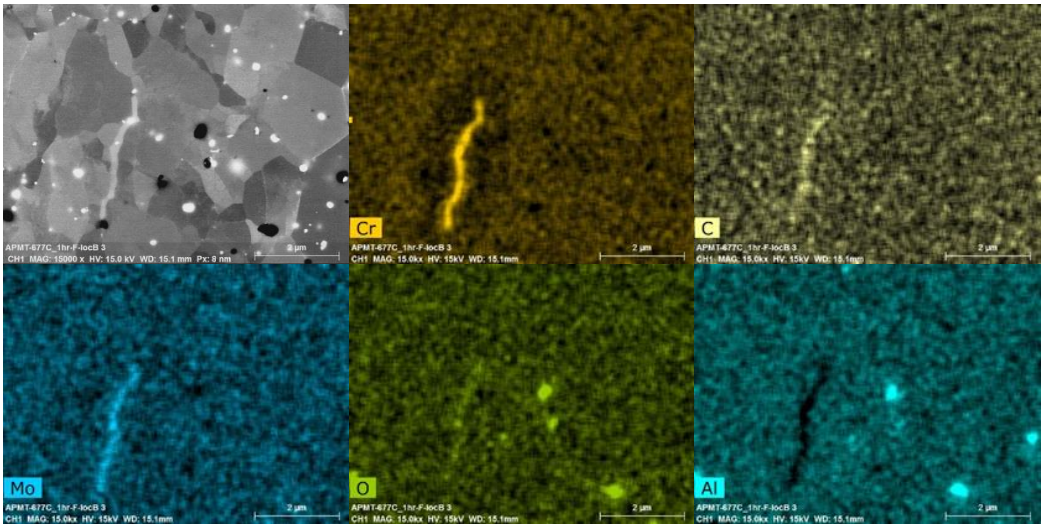  |
| C26M | 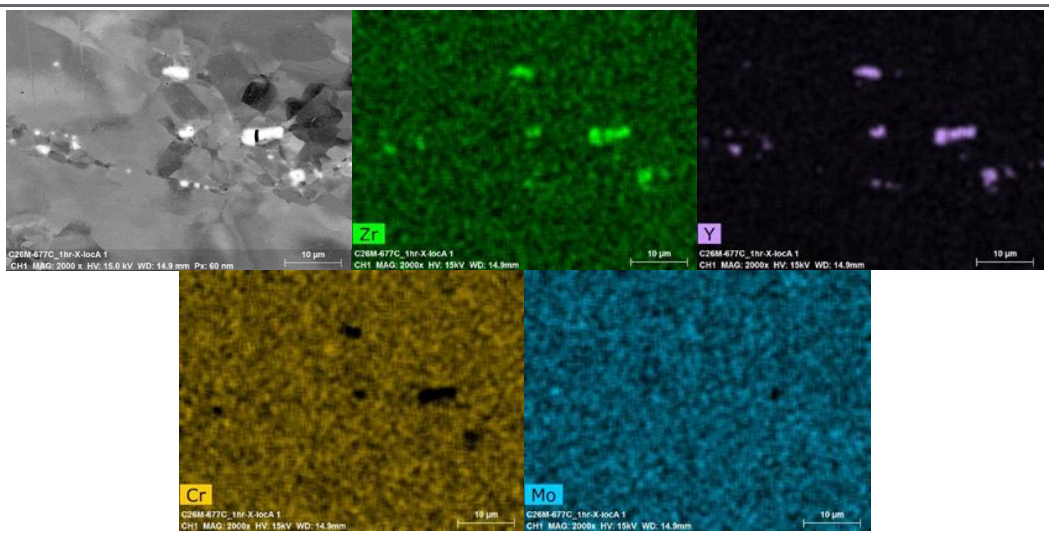  |

**Figure 6**. Thermally treated (677°C for 2h) microstructures and composition of 304H SS, and APMT at X15,000 and C26M at X2000 magnification.

| Alloy | 732°C, 1h, X15,000 |
|---|---|
| 304HSS | 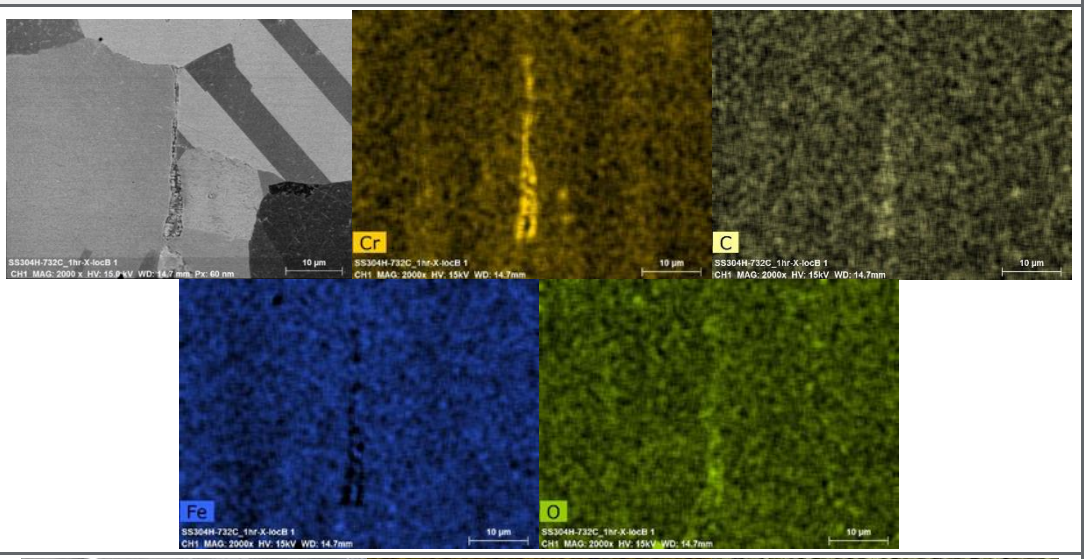 |
| APMT | 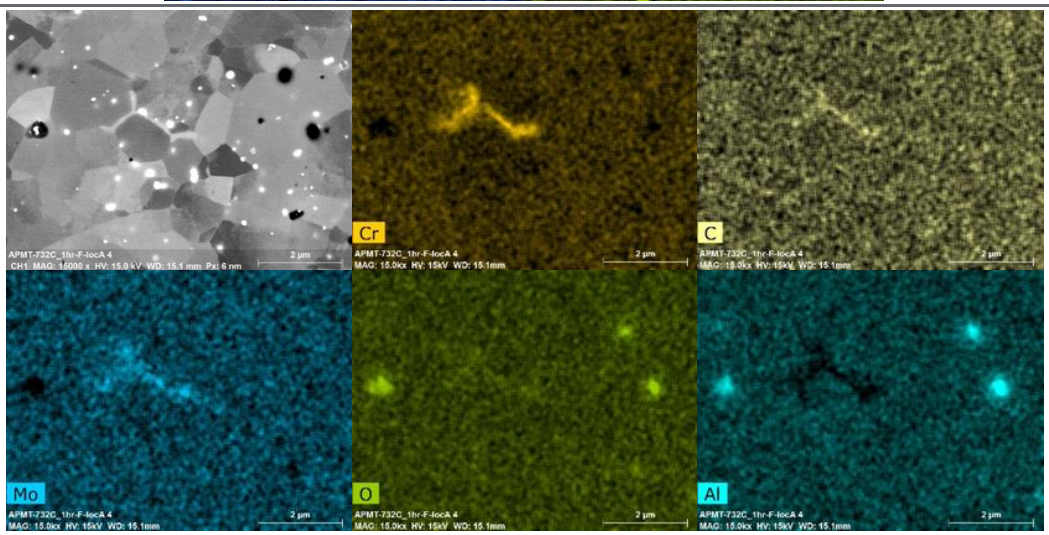 |
| C26M | 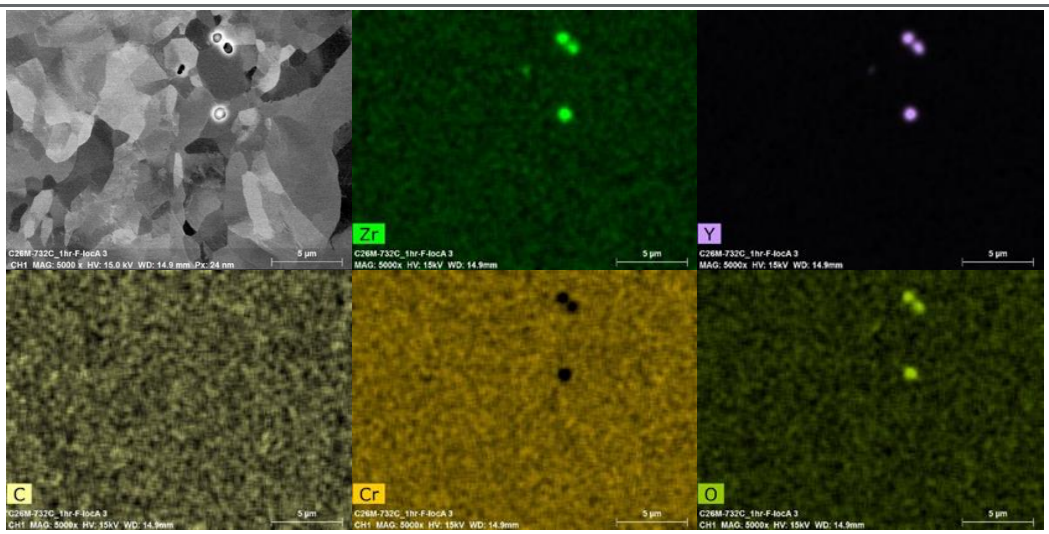 |

**Figure 7**. Thermally treated (732°C for 1h) microstructures and composition of 304H SS at X2000, C26M at X5000 and APMT at X15,000 magnification.

In Figure 6, the intensity levels on O maps for the same Cr and Mo-rich features in corresponding maps, are weak and not at the similar levels as with features on O maps that correspond to features on Al maps. It is more likely that O is part of aluminum oxide or pores that were filled with polishing media and are not carbides. Figures 4, 5, and 6 show that C26M has the cleanest microstructure, with almost no precipitates rich in Cr or C. Some of the globular nano-sized precipitates are rich in Zr and Y.

**Welding of IronClad (FeCrAl) Alloys**

During the assembly of the fuel rods, the tubes containing the fuel pellets must be welded hermetically to caps at both ends. In general, for zirconium alloys, the bottom weld (before the insertion of the pellets) is performed using TIG welding and, after the fuel insertion, the final weld is performed using pressure resistance welding (PRW). Global Nuclear Fuels (GNF) performed welding trials for FeCrAl IronClad using both methods and found both methods satisfactory for the welding. This is an ongoing work, and therefore, only TIG-welded samples are briefly discussed below.

Figures 8 and 9 show montages of TIG welds in APMT and C26M alloys, respectively. The tube wall thickness of APMT was 0.6 mm and that of C26M was 0.4 mm. Both materials weld well using TIG welding method. The figures show some grain growth at the TIG weld seam, especially for C26M material. However, the welded joints are found to be free from cracks, oxidation or porosity, and fully hermetic. In addition, high-magnification SEM images taken from weld and heat affected zones, show absence of chromium carbide formation at grain-boundaries (i.e., no sensitization) during the TIG welding process.

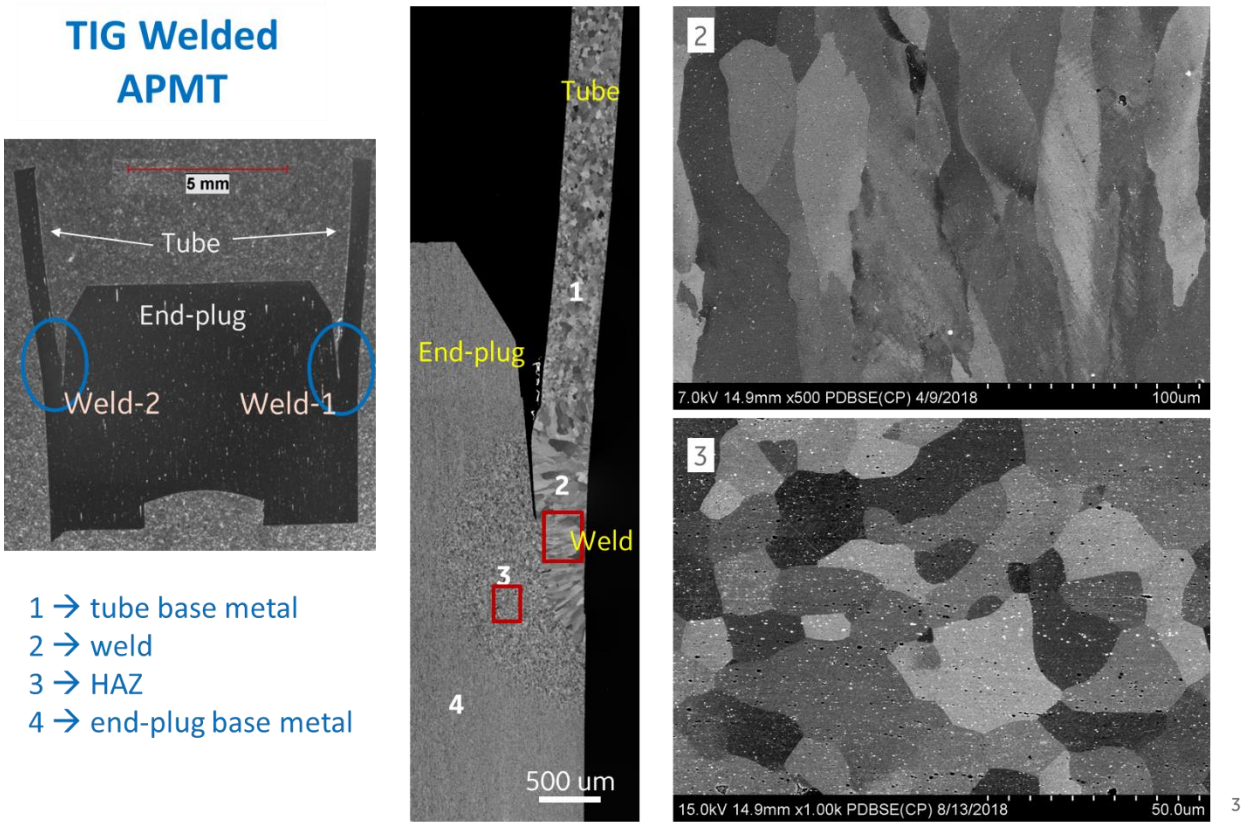


**Figure 8**: Series of images (Optical macro- and SEM micrographs) from TIG welded APMT alloy.

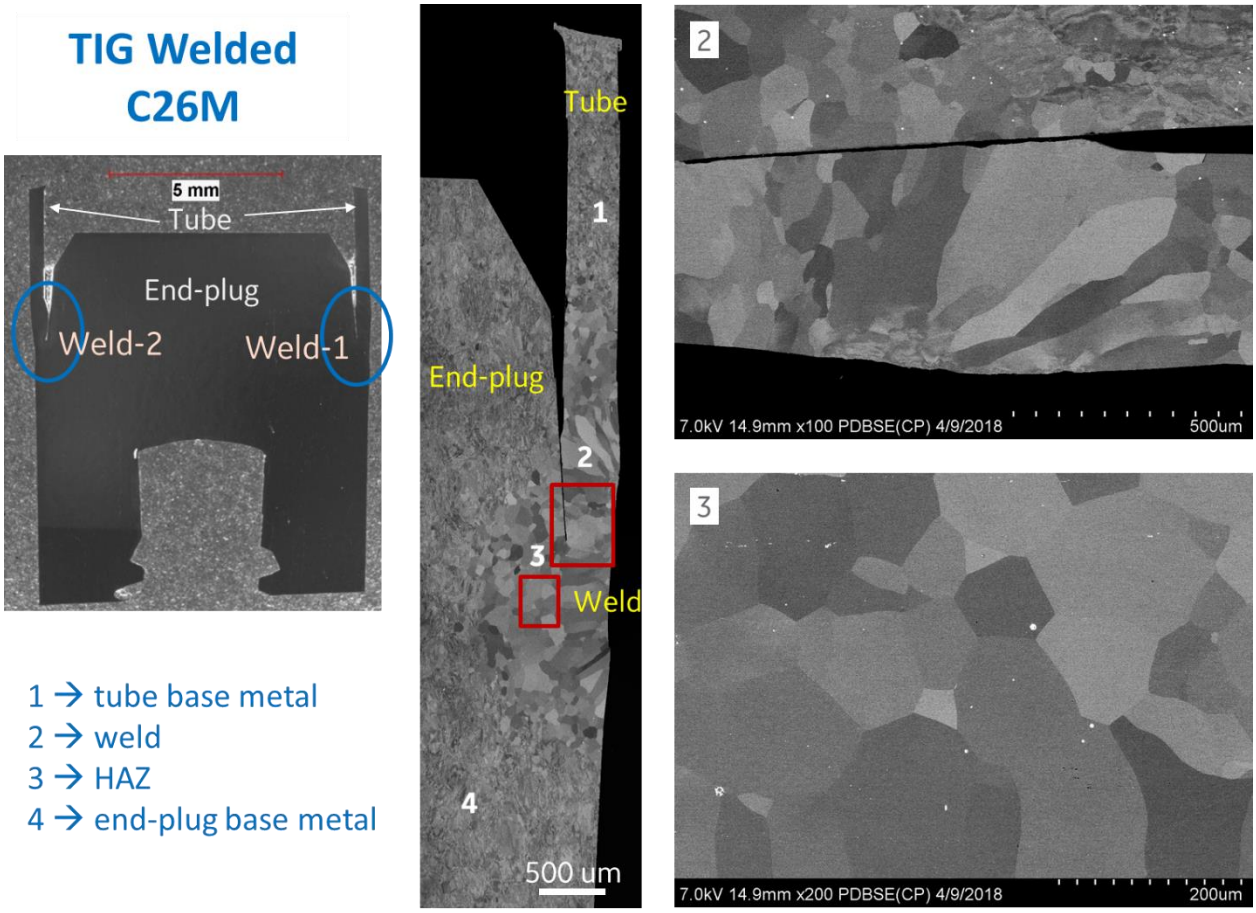


**Figure 9**: Series of images (Optical macro- and SEM micrographs) from TIG welded C26M alloy.

## SUMMARY AND CONCLUSIONS

1. IronClad materials such as APMT and C26M suffer no grain-boundary sensitization (i.e., no Cr carbide precipitation at grain boundaries and formation of Cr depletion regions) during thermal exposures at 677°C and 732°C. In contrast, higher carbon austenitic Type 304H SS, which was used as benchmark material for this study, showed sensitization by the precipitation of secondary carbides at the grain boundaries after thermal exposures in the range 650-750°C.
2. Powder metallurgy alloy APMT contains the largest volume of precipitates of the three alloys, such as carbides rich in Cr and Mo, as well as sub-micron globular oxides rich in Al, Hf, Zr and Y. Traditionally melted alloy C26M was the cleanest material even after thermal treatment, containing only sporadic nano-sized globular Zr and Y rich oxides.
3. Both IronClad alloys (APMT and C26M) are weldable by the TIG method, without cracks, porosity or internal oxidation in the weld seam.

**ACKNOWLEDGEMENTS**

This material is based upon work supported by the Department of Energy [National Nuclear Security Administration] under Award Number DE-NE0008221. The financial support of Global Nuclear Fuels is gratefully acknowledged. This report was prepared as an account of work sponsored by an agency of the United States Government. Neither the United States Government nor any agency thereof, nor any of their employees makes any warranty, express or implied, or assumes any legal liability or responsibility for the accuracy, completeness, or usefulness of any information, apparatus, product, or process disclosed, or represents that its use would not infringe privately owned rights. Reference herein to any specific commercial product, process or service by trade name, trademark, manufacturer, or otherwise does not necessarily constitute or imply its endorsement, recommendation, or favoring by the United States Government or any agency thereof. The views and opinions of authors expressed herein do not necessarily state or reflect those of the United States Government or any agency thereof.

**REFERENCES**

1. K. A. Terrani, “Accident Tolerant Fuel Cladding Development: Promise, Status, and Challenges,” JNM, 10.1016/j.jnucmat.2017.12.043, American Nuclear Society (2018).
2. F. Nagase, K. Sakamoto, and S. Yamashita, “Performance degradation of candidate accident-tolerant cladding under corrosive environment,” Corros. Rev 2017; 35(3): 129–140.
3. R. B. Rebak, M. Larsen, and Y.-J. Kim, “Characterization of oxides formed on iron-chromium-aluminum alloy in simulated light water reactor environments,” Corrosion Reviews 2017 DOI 10.1515/corrrev-2017-0011
4. R. B. Rebak “Versatile Oxide Films Protect FeCrAl Alloys Under Normal Operation and Accident Conditions in Light Water Power Reactors,” JOM., (2018) 70: 176. https://doi.org/10.1007/s11837-017-2705-z.
5. IAEA Nuclear Energy Series, “Stress Corrosion Cracking in Light Water Reactors: Good Practices and Lessons Learned,” No. NP-T-3.13, (Vienna, September 2011).
6. P. L. Andresen, R. B. Rebak and E. J. Dolley, “SCC Resistance of Irradiated and Unirradiated High Cr Ferritic Steels,” Paper 3760, Corrosion/2014 Conference (NACE International, Houston, TX 2014).
7. A. P. Majidi and M. A. Streicher, “The Double Loop Reactivation Method for Detecting Sensitization in AISI 304 Stainless Steels,” Corrosion, 40, 584 (1984).
8. M. E. Gonzalez, M. A. Kappes, M. A. Rodriguez, P. Bozzano, R. M. Carranza, and R. B. Rebak, “Optimization of the Double Loop Electrochemical Potentiokinetic Reactivation Method for Detecting Sensitization of Nickel Alloy 690,” Corrosion, 74, 2, (2018).